

Towards Autonomous Phytopathology: Outcomes and Challenges of Citrus Greening Disease Detection through Close-range Remote Sensing

Suproteem K. Sarkar^a, Jnaneshwar Das^a, Reza Ehsani^b, Vijay Kumar^a

^aGRASP Laboratory, University of Pennsylvania
{sarkarsu,djnan,kumar}@seas.upenn.edu

^bCitrus Research and Education Center, University of Florida
ehsani@ufl.edu

Abstract— Unmanned aerial vehicles (UAVs) have the potential to significantly impact early detection and monitoring of plant diseases. In this paper, we present preliminary work in developing a UAV-mounted sensor suite for detection of citrus greening disease, a major threat to Florida citrus production. We propose a depth-invariant sensing methodology for measuring reflectance of polarized amber light, a metric which has been found to measure starch accumulation in greening-infected leaves. We describe the implications of adding depth information to this method, including the use of machine learning models to discriminate between healthy and infected leaves with validation accuracies up to 93%. Additionally, we discuss stipulations and challenges of use of the system with UAV platforms. This sensing system has the potential to allow for rapid scanning of groves to determine the spread of the disease, especially in areas where infection is still in early stages, including citrus farms in California. Although presented in the context of citrus greening disease, the methods can be applied to a variety of plant pathology studies, enabling timely monitoring of plant health—impacting scientists, growers, and policymakers.

I. INTRODUCTION

Robotics and automation provide novel approaches for precision agriculture—particularly for crop harvesting, seeding, de-weeding, yield estimation, phenotyping, and stress detection [1-6]. A newly emerging field is the application of robotics and machine learning methods to phytopathology [7,17]. Plant diseases routinely affect crop health, resulting in significant losses to the economy. Robotic sampling has the potential to help growers and plant pathologists detect and monitor the onset and progression of diseases, allowing for timely treatment and quarantining. Potential threats in phytopathology span a wide range of diseases, including apple scab, pecan scab, peach scale, and fire blight. Each disease has unique characteristics that require complex sensing and lab analysis for detection. In this work, we summarize the development and evaluation of an imaging system suitable for use with autonomous unmanned aerial vehicles (UAVs), for detection of citrus greening disease, also known as huanglongbing (HLB). HLB leads trees to yield green, misshapen, and bitter fruit, rendering them unmarketable and posing a significant challenge to the citrus industry. The disease is reported to be caused by

Candidatus Liberibacter asiaticus, which is transmitted by the Asian citrus psyllid [8]. HLB has been present in Florida since 2005 [8], and in the past three years has been detected in California [9] and Texas [10]. The infection also affects groves in Asia and South America [11].

An early symptom of citrus greening is starch accumulation in leaves, which is thought to be caused by phloem blockages. Pourreza et al. proposed a vision-based sensor that can detect HLB by measuring leaf starch's reflectance of rotated polarized light [17,18]. Their research found that placing polarizing filters in perpendicular orientations in front of a light source and camera could lead to differentiation between HLB-infected and healthy leaf samples.

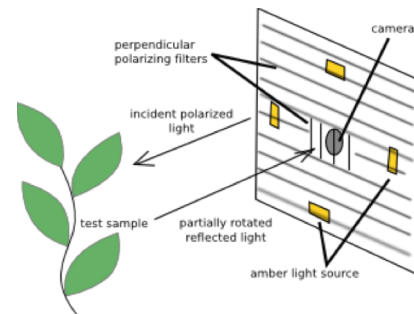


Figure 1: HLB detection methodology proposed by Pourreza et al. [17]. An array of high power amber LEDs with a polarizing filter illuminates the target leaves. A camera with a perpendicular filter measures intensity of rotated light.

The remote sensing methodology developed by Pourreza et al. that uses spectrally selective light is ideal for deployment on UAVs, potentially providing agronomists with the capability of selective and repeatable monitoring of HLB disease progression. However, one issue with a solely reflectance-based sensor is a lack of depth-invariance, since intensity decreases as distance increases through an inverse-square relationship. Depth-invariance can allow a sensor to account for fluctuations in distance to trees when scanning across a grove using an unmanned aerial vehicle (UAV) or ground vehicle. We propose an imaging system that measures

both reflectance of rotated polarized light, and distance. This enhanced sensing modality can allow depth-invariant sensing of starch accumulation in order to determine HLB infection.

Our work makes the following three contributions. First, we present a lightweight imaging system with an onboard spectrally selective light source for citrus greening disease detection. By using an RGB-D sensor instead of a standard camera proposed in prior work, we are able to use both pixel intensity and depth in acquired imagery to develop a depth-invariant HLB classifier. Second, we present results of experiments at a greenhouse and in the field. A comparison of various classifiers is presented, with detection accuracy as high as 93%. Finally, we carried out the first night-time flights with the *active spectrally-selective illumination imaging system* for disease detection. The UAV trials serve as a proof of concept, opening up the arena for application of UAVs in plant pathology studies.

The outline of the paper is as follows. In Section II, we discuss the imaging system and experiment design. In Section III, we discuss evaluation results of discriminative machine learning models, on data acquired at a greenhouse and at an orange grove in Lake Alfred, Florida. Additionally, we discuss the outcome of the UAV flight with the imaging system onboard, and summarize the implications and challenges of airborne deployment of the imaging system. Finally, we present future directions and conclude in Section IV.

II. SYSTEMS AND METHODS

In this section, we discuss the fabrication and assessment of the prototype imaging system, and describe the experiment design for greenhouse and field tests.

A. Background

Prior work in HLB detection using close-range remote sensing by Pourezza et al. has established the use of polarized amber light (590nm) on test plant leaves, followed by sensing with a camera with a perpendicular polarizing film. Figure 1

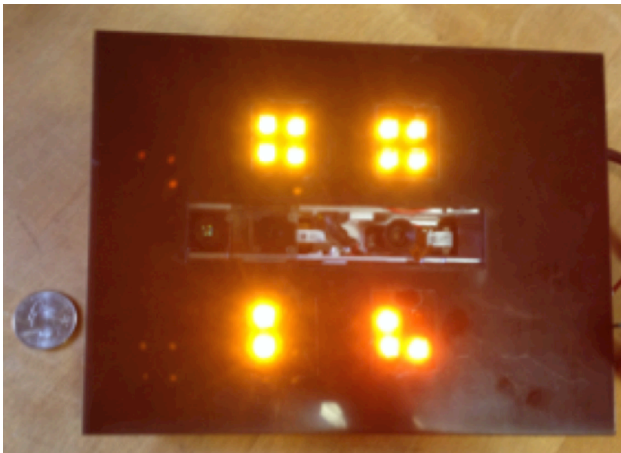


Figure 2: Prototype sensor package proposed in this work, consisting of an RGB-D sensor and amber LEDs. The camera and LEDs are covered with polarizing film oriented in perpendicular directions.

shows an illustration of the sensing methodology.

B. Prototype Design

We made modifications to the sensing methodology to allow for depth-invariance. Figure 2 shows the first prototype of our sensor suite. An ASUS Xtion PRO LIVE RGB-D sensor was used to collect intensity and depth data. This sensor consists of a 640x480 RGB camera that can acquire images at 30 frames per second, and an infrared projector and sensor that measures depth without external lighting. For preliminary trials, the RGB camera on the sensor was covered with a polarizing film (Edmund Optics Visible Linear Polarizing Laminated Film), and samples were illuminated with 591nm LEDs (LED Engin LZ1-00A100) covered with a polarizing film perpendicular to the film in front of the camera. Sensor messages for depth and intensity were processed and stored using the Robot Operating System (ROS) [15]. To test the sensor, one branch on each of three Valencia sweet orange trees was girdled to induce starch accumulation [19]. The orange trees were imaged with the preliminary sensor package over a period of six months. Though girdling may lead to starch accumulation, the composition of the starch produced is different than the composition of starch found in HLB-infected leaves [20]. In order to allow for more accurate ground truthing, the sensor was then tested on HLB-infected specimens.

C. Scale Up

The second iteration of the sensor package was developed to allow for sensing at greater distances and scalability to a UAV platform. Twelve narrow-band 600nm LEDs (JDM ASTAR AX-2835) were used for amber illumination as a baseline. As high-power narrow-band LEDs are not widely commercially available, we also tested two broader-spectrum 20W LEDs centered at 590nm (DX Square LED Yellow Light Module). The reflected light from the broader-spectrum light source was analyzed by using red channel information from the RGB camera. All the light sources were covered with polarizing film perpendicular to the film covering the



Figure 3: Updated sensor package, mounted on a DJI S800 hexacopter. Both a narrow-band amber and broad-spectrum light source were used. The broad-spectrum light source was processed through the red channel of the RGB-D camera. The sensor also consisted of two grayscale cameras and a 3DRobotics Pixhawk autopilot system.

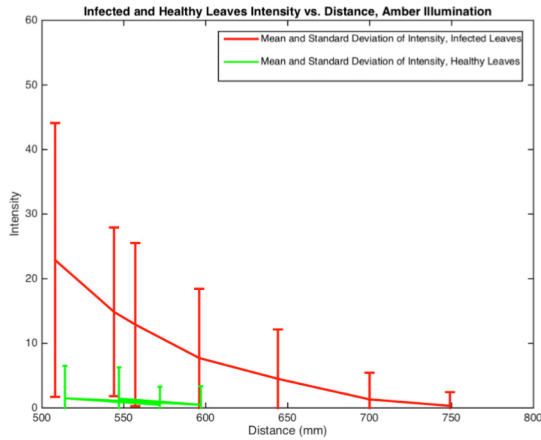


Figure 4: Overview plot of intensity vs. depth for infected and healthy leaves illuminated by amber light, with means and standard deviations of combined leaf data taken across depth bins. Infected leaves were on average 5.11 times as bright as healthy leaves, though the difference was apparent only at low distances.

RGB-D camera. The package also employed two grayscale cameras (mvBlueFOX-MLC202bG), covered with polarizing film parallel and perpendicular to the light sources. The sensor was mounted to a UAV (DJI S800 hexrotor) for handheld and flight-based experiments at orange groves of University of Florida’s Citrus Research and Education Center in Lake Alfred, Florida. GPS and IMU information were recorded using the 3DRobotics Pixhawk autopilot system. The total sensor package weighed 1.10 kg, and measured 102cm x 46cm x 21cm. The LEDs were powered by a 2700 mAh 11.1 V lithium polymer battery, and an Intel i5 computer collected the data from the sensor and autopilot system.

III. RESULTS

A. Individual Leaf Trials

To acquire a ground truth dataset to train the HLB classifier, individual leaves were imaged through the RGB-D

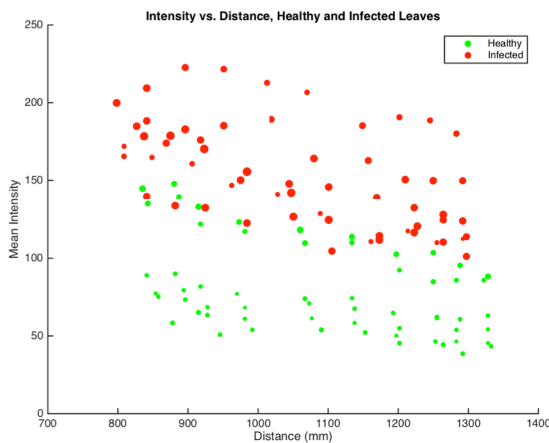


Figure 6: Detailed plot of mean intensity vs. distance of healthy and infected leaves. The size of each point corresponds to the standard deviation of intensity for individual leaves.

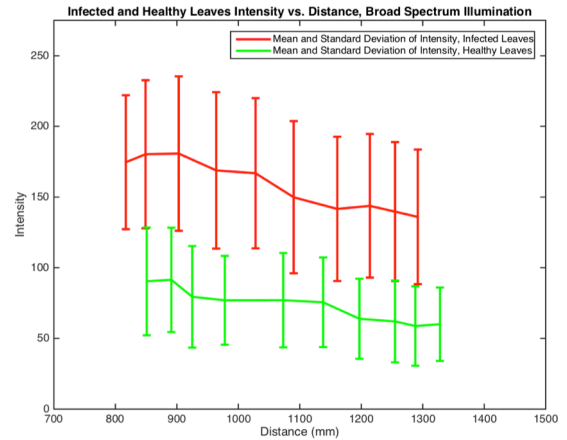


Figure 5: Overview plot of intensity vs. depth for infected and healthy leaves illuminated by broad spectrum light, with means and standard deviations of combined leaf data taken across depth bins. Infected leaves were on average 2.04 times as bright as healthy leaves, though signals were detectable at higher distances.

camera’s red channel using amber light and broad-spectrum light. In order to avoid interference from external light sources, the experiments were carried out in a dark room. Leaf data were extracted from images through masking, and intensity and depth were recorded for all pixels in the leaf masks. The mean and standard deviation of intensity values were recorded for leaves from healthy and infected trees, for individual depth bins. Mean and standard deviation were isolated, as they had been shown in previous work to predict HLB infection at fixed distances. The median distance was adapted as a new feature as it would show the effects of the inverse relationship between intensity and distance.

Sensor images acquired using amber illumination showed the greatest distinction between infected and healthy leaves. In a trial with 60 samples per leaf type, intensity means for HLB-infected leaves were 5.11 times higher than means for healthy leaves averaged across distances. However, amber

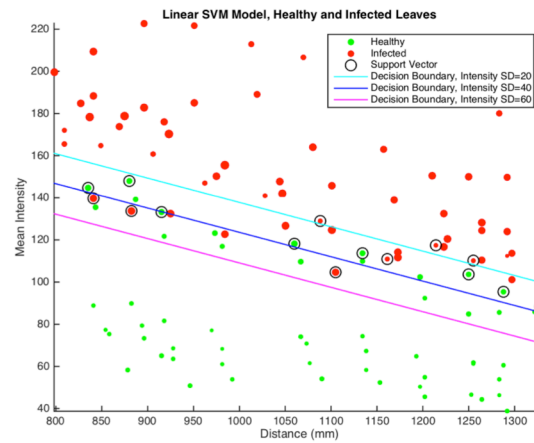


Figure 7: Linear SVM decision boundaries for classifying healthy and infected leaves. Note the downward shift in the boundary as standard deviation increases.

<i>Comparison of Machine Learning Methods for Healthy and Infected Leaf Classification</i>	Validation Accuracy	False Positive Rate	False Negative Rate
<i>Linear SVM</i>	93.3%	8.3%	5.0%
<i>k-Nearest Neighbor</i>	90.0%	1.7%	18.3%
<i>Coarse Gaussian SVM</i>	88.3%	11.7%	11.7%
<i>Standard Gaussian SVM</i>	93.3%	3.3%	10.0%
<i>Simple Decision Tree</i>	90.8%	11.7%	6.7%
<i>Complex Decision Tree</i>	91.7%	10.0%	6.7%

Figure 8: Table of validation accuracy, false positive rate, and false negative rate for machine learning methods used to classify infected and healthy leaves. The data were calculated through 5-fold cross validation. Linear SVM and Gaussian SVM had the highest validation accuracies, while linear SVM had the lowest false negative rate.

illumination produced relatively low intensity counts, even for distances as close as 700mm. These low intensity values pose a problem for scale-up, as the sensor mounted on a UAV would need to image trees from larger distances. In addition, noise effects may have come into play with lower intensity values.

To allow for higher levels of illumination, which is important for sensing from farther distances aboard UAVs, higher-power LEDs were tested with the sensor. Although the higher-power LEDs were centered at 590nm, they had broader spectra than the amber LEDs. In order to account for

this difference, red channel data from the RGB-D camera were used for intensity measurements. Intensity counts for HLB-infected leaves measured with broad-spectrum illumination were an average of 2.04 times higher than values for healthy leaves across distances.

B. Prediction Algorithms

Results from the broad spectrum illumination trials were used to develop models to classify healthy and infected leaves. Image masks were taken of individual leaves to gather intensity and depth information for individual pixels. Median

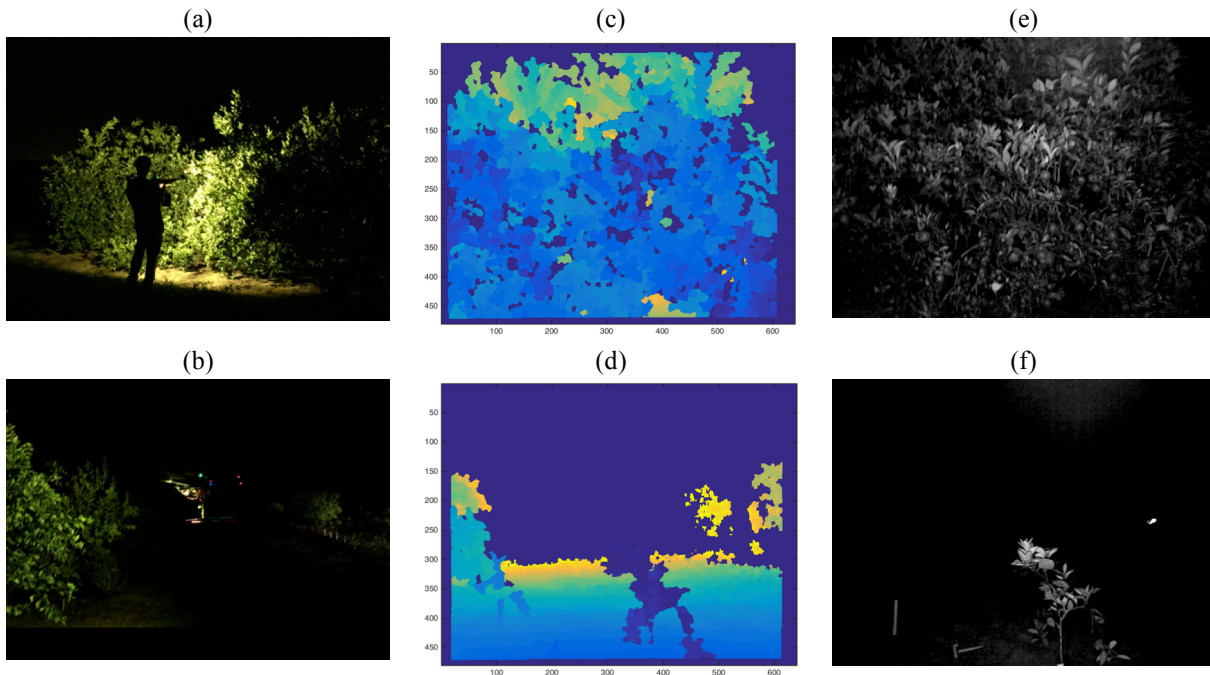


Figure 9: (a) Sensor in use for handheld sensing. (b) The sensor in flight. The UAV-mounted sensor was used to image trees in the orange grove from the side. Reset, or recently planted, trees were used as identifiers of healthy trees. (c) through (f) show images acquired by the RGB-D camera. Scaled depth images of (c) infected and (d) reset trees. Intensity images of (e) infected and (f) reset trees.

depth, mean intensity and standard deviation of intensity features were extracted from each leaf.

Linear support vector machine (SVM), Gaussian SVM, k-nearest neighbor and decision tree models were used to classify healthy and infected leaves using distance and intensity data. Gaussian SVM was conducting using coarse ($4 * \sqrt{\# \text{ Predictors}} = 6.9$) and standard ($\sqrt{\# \text{ Predictors}} = 1.7$) kernel scales. Both complex (maximum 20 splits) and simple (maximum 4 splits) decision trees were evaluated.

5-fold cross-validation was used to assess the validation accuracies of the classification methods. Linear SVM and fine Gaussian SVM had the highest validation accuracies of all the models, at 93.3%, while linear SVM also had the lowest false negative rate, at 5.0%.

Mean intensity values for the decision boundary generated through the linear SVM model decreased as median distance and standard deviation of intensity increased. The inverse relationship between distance and intensity can be attributed to the documented inverse relationship between the two properties.

The inverse relationship between mean intensity and standard deviation of intensity poses another question. One explanation we propose is the potential for unequal starch accumulation across individual infected leaves. The resulting varying intensity values on infected leaves could explain why in general, given similar mean intensities, infected leaves imaged by the sensor displayed higher standard deviation intensities than healthy leaves. Further work studying starch accumulation distributions in greening-infected leaves will have to be conducted to explore this property in more detail.

C. UAV Scale Up

Scaling up the sensor package to a UAV platform presents novel considerations and challenges. In this section, we describe the implications of mounting a vision-based greening detection package on a UAV.

The most significant challenge we aimed to address with this work was the problem of fluctuations in distance between the sensor and leaves. Since intensity varies with distance, an intensity-dependent model is undesirable, as decision boundaries would be effective only at distances for which training data are available. Adding depth as a feature allows for more effective classification across a wide range of distances.

The ability of the RGB-D sensor to acquire depth information for individual points also facilitates accurate classification by allowing for discrimination of distances within an individual image; for example, the sensor can distinguish clusters of leaves at different distances from the camera within the same frame. Though depth-invariance was used in this work in the context of scale-up to a UAV, the principle is also important for sensing through other platforms, including handheld and ground vehicle-based setups.

Another challenge posed by aerial imaging is lower intensity counts overall at the relatively larger distances to trees used during UAV operation. The amber lights used in this work exhibited low intensity counts across the board, and leaves were barely detectable after 70 cm. Some of these constraints were due to the limitations of RGB-D camera—namely a lack of manual settings for higher exposure through ROS. Using a more configurable camera, calibrating it with the RGB-D depth sensor, and adjusting the exposure appropriately could address this issue.

However, in order to image at even larger distances, there is a need for higher-power light sources for illumination. The 20W LEDs used in this work provided more reliable illumination at distances up to 1.5 m, though future experiments may want to consider even more powerful light sources. One important constraint to consider for the extent of illumination is saturation of the polarizing film.

In addition, a key concept to explore further is the degree of spectral selectivity that is optimal for discrimination between healthy and infected specimens. This work found that the difference in intensity between infected and non-infected leaves was more pronounced with a narrow-band light source than with a broader-spectrum source imaged through a red channel, though the broader-spectrum light source could receive signals from larger distances. Future directions in this area include testing with light sources of varying spectrum sizes, and documentation of the effects of adding a narrow-band filter to the camera in lieu of placing the burden of spectral selectivity solely on the light source.

Leaf detection also poses a challenge at the larger distances to trees employed during UAV flight. Though work has been conducted on leaf detection using RGB-D sensors [21], individual detection can be impractical at the distances used during flight. Further work on generalizing the individual leaf data to clusters or regions that can be observed on trees in a grove could allow for more accurate discrimination at a larger scale.

Thus, three major improvements would allow for more efficient UAV-based detection of citrus greening. Higher-power light sources facilitate imaging at larger distances. Cameras with manual exposure allow for greater accuracy across sample types. Finally, ground truthing on clusters of leaves can enable more accurate discrimination at larger scales.

IV. CONCLUSIONS AND FUTURE DIRECTIONS

This paper described an imaging system with potential for airborne detection of citrus greening disease. Controlled evaluation was carried out on leaf samples from a greenhouse, followed by validation on diseased and healthy citrus trees at an orange grove in Lake Alfred, Florida. The key contributions of our work were an extension of an existing methodology for citrus greening disease detection to depth-invariant sensing and a discussion of the implications of scaling up such a system to a UAV platform.

Additionally, we presented the first night-time UAV flight with the system on board, scanning diseased and healthy plants from the side at an altitude under two meters. By using an RGB-D sensor, we were able to demonstrate the use of intensity and depth information for individual pixels as a means for disease detection.

We also extended previous work by testing broader-spectrum illumination, which allowed for sensing at larger distances. Though the broader-spectrum illumination methodology displayed less distinction between infected and healthy specimens, support vector machine classifiers were able to distinguish between healthy and infected leaves at an accuracy of 93% at up to 1.4 m using the broad-spectrum light source.

We then described the implications and modifications considered during the scale-up to our first UAV trial. Operating the sensor package at a larger scale brought up new issues, for which we outlined future directions that could allow for more effective sensing and discrimination.

As citrus greening threatens orange production worldwide, there is a pressing need for technology that can make early detection and quarantining more efficient and accessible. By applying techniques from robotics and machine learning to precision agriculture, this work seeks to help combat the spread of the disease.

ACKNOWLEDGMENTS

We gratefully acknowledge the support of USDA grant 2015-67021-23857 under the National Robotics Initiative, ONR grant N00014-07-1-0829, NSF grant IIP-1113830, and the Berkman Opportunity Fund at the University of Pennsylvania. We also acknowledge Geraldine Lavin and Tracylea Byford at the University of Pennsylvania Greenhouse for supporting initial sensor trials and maintaining the citrus trees.

REFERENCES

- [1] J. Das, G. Cross, C. Qu, A. Makineni, P. Tokekar, Y. Mulgaonkar, V. Kumar. "Devices, Systems, and Methods for Automated Monitoring enabling Precision Agriculture". IEEE International Conference on Automation Science and Engineering (CASE), pp. 462-469, 2015
- [2] M. Bryson, A. S. Reid, F. T. Ramos, and S. Sukkarieh, "Airborne Vision-based Mapping and Classification of Large Farmland Environments," *Journal of Field Robotics*, vol. 27, no. 5, pp. 632–655, 2010.
- [3] P. J. Zarco-Tejada, J. A. Berni, L. Suarez, and E. Fereres, "A new era in remote sensing of crops with unmanned robots," *SPIE Newsroom*, pp. 2–4, 2008.
- [4] U. Weiss, P. Biber, S. Laible, K. Bohlmann, and A. Zell, "Plant Species Classification Using a 3D LIDAR Sensor and Machine Learning," in *Machine Learning and Applications (ICMLA), 2010 Ninth International Conference on*, Dec 2010, pp. 339–345.
- [5] S. Singh, M. Bergerman, J. Cannons, B. Grocholsky, B. Hamner, G. Holguin, L. Hull, V. Jones, G. Kantor, H. Koselka, *et al.*, "Comprehensive Automation for Specialty Crops: Year 1 results and lessons learned," *Intelligent Service Robotics*, vol. 3, no. 4, pp. 245–262, 2010.
- [6] T. Bakker, K.A. van, J. Bontsema, J. Mller, and G.S. van, "Systematic design of an autonomous platform for robotic weeding," *Journal of Terramechanics*, vol. 47, no. 2, pp. 63 – 73, 2010.

- [7] L. Techy, D.G. Schmale, and C.A. Woolsey, "Coordinated aerobiological sampling of a plant pathogen in the lower atmosphere using two autonomous unmanned aerial vehicles. *Journal of Field Robotics* 27: 335-343, 2010
- [8] Aphis.usda.gov, 'USDA APHIS | Citrus Greening', 2015. [Online]. Available: http://www.aphis.usda.gov/wps/portal/aphis/ourfocus/plant_health/sa_domestic_pests_and_diseases/sa_pests_and_diseases/sa_plant_disease/sa_citrus/ct_citrus_greening!/ut/p/a/1/. [Accessed: 17- Aug-2015].
- [9] Cdfa.ca.gov, 'CDFA > Public Affairs > Press Release', 2015. [Online]. Available: http://www.cdfa.ca.gov/egov/Press_Releases/Press_Release.asp?PRnum=15-031. [Accessed: 17- Aug- 2015].
- [10] O. El-Lissy, "APHIS Confirms Citrus Greening (Candidatus *Liberibacter asiaticus*) in Mission, Texas," *USDA APHIS*, 2013.
- [11] Aphis.usda.gov, 'USDA APHIS | Citrus Greening Background', 2015 [Online].
- [12] O.W. Liew, P.C.J. Chong, B.Li, and A.K.Asundi, "Signature optical cues: emerging technologies for monitoring plant health," *Sensors*, vol. 8, no. 5, pp. 3205–3239, 2008.
- [13] J. Berni, P. Zarco-Tejada, L. Suarez, and E. Fereres, "Thermal and Narrowband Multispectral Remote Sensing for Vegetation Monitoring From an Unmanned Aerial Vehicle," *Geoscience and Remote Sensing, IEEE Transactions on*, vol. 47, no. 3, pp. 722–738, March 2009.
- [14] A. Jaakkola, J. Hyyppä, A. Kukko, X. Yu, H. Kaartinen, M. Lehtomäki, and Y. Lin, "A low-cost multi-sensoral mobile mapping system and its feasibility for tree measurements," *ISPRS Journal of Photogrammetry and Remote Sensing*, vol. 65, no. 6, pp. 514 – 522, 2010.
- [15] M. Quigley, K. Conley, B. P. Gerkey, J. Faust, T. Foote, J. Leibs, R. Wheeler, and A. Y. Ng, "ROS: an open-source Robot Operating System," in *ICRA Workshop on Open Source Software*, vol. 3, no. 3.2, 2009, p. 5.
- [16] R. Gade and T. B. Moeslund, "Thermal cameras and applications: A survey," *Machine Vision and Applications*, vol. 25, no. 1, pp. 245–262, Jan. 2014.
- [17] A. Pourreza, W.S. Lee, R. Ehsani, J.K. Schueller, E. Raveh, "An optimum method for real-time in-field detection of Huanglongbing disease using a vision sensor", *Computers and Electronics in Agriculture*, Volume 110, Pages 221-232, 2015.
- [18] A. Pourreza, W. S. Lee, E. Raveh, R. Ehsani, E. Etxeberria, "Citrus Huanglongbing Disease Detection Using Narrow Band Imaging and Polarized Illumination," *Transactions of the ASABE* 2014, 57(1): 259-272 , 2014.
- [19] A. Schaffer, K. Liu, E. Goldschmidt, C. Boyer and R. Goren, 'Citrus Leaf Chlorosis Induced by Sink Removal: Starch, Nitrogen, and Chloroplast Ultrastructure', *Journal of Plant Physiology*, vol. 124, no. 1-2, pp. 111-121, 1986.
- [20] P. Gonzalez, J. Reyes-De-Corcuera, and E. Etxeberria, "Characterization of leaf starch from HLB-affected and unaffected-girdled citrus trees," *Physiological and Molecular Plant Pathology*, vol. 79, pp. 71-78, 2012.
- [21] C. Xia, L. Wang, B.-K. Chung, and J.-M. Lee, "In Situ 3D Segmentation of Individual Plant Leaves Using a RGB-D Camera for Agricultural Automation," *Sensors*, pp. 20463–20479, 2015.